Referee comment #1:

In this article, the authors present a study of burning emission in China using MODIS inputs and an empirical fire radiative energy method. The fire emission issue in China is an important one due to its complexity caused by the rapid social development. This paper is well written. But There are still some issues to be discussed.

Response: We appreciate the review's comments, which indeed help us to improve the manuscript much.

1. The land cover

Globcover 2009 is used in this study. However, during the study period, China experienced dramatic changes, including urban expansion brought about by rapid urbanization, as well as returning farmland to forests and grasslands. The emission factors are dependent on the type of vegetation. Therefore, at 1km resolution level, large emission uncertainties may occur due to the biases in land cover data. Maybe annual land cover data is a better choice.

Response: Accepted. MODIS land cover product (MCD12Q1) provide annual land cover data, but the spatial resolution (500 m) is relatively coarse. Because the open fire size is often small in China, we used GlobelLand30 dataset with 30 m resolution (covering year 2000 and 2010) instead of GlobCover2009 in the revised manuscript. The land cover types are characterized by GlobeLand30-2000 for years 2003–2005 and GlobeLand30-2010 for years 2006–2017.

Revisions: (Page 6, Line 9) "The GlobeLand30 dataset maps global land cover at 30 m spatial resolution in two base years (2000 and 2010) (Chen et al., 2017b), as shown in Fig S2 (small islands in the South China Sea are not included). GlobeLand30 data are generated by multispectral images derived from Landsat TM, ETM+ and Chinese Environmental Disaster Alleviation Satellite (HJ-1). The result of accuracy assessment shows that the overall accuracy of GlobeLand30 reaches 83.5 %. GlobeLand30 dataset consists of 10 land cover types, namely cultivated land, forest, grassland, shrubland, wetland, water bodies, tundra, artificial surfaces, bareland, permanent snow and ice. In this study, the land cover types are characterized by GlobeLand30-2000 for years 2003–2005 and GlobeLand30-2010 for years 2006–2017. We combined the land-cover map of China and the latitude and longitude data of fire count in MOD14/MYD14 to determine the biomass fuel types. For instance, if a fire count locates in cropland area, it will be considered as a crop residue burning event."

2. Seasonal patterns

The authors did not show much about seasonal patterns of the results, which is very effective in evaluating the results. Due to the impact of the monsoon climate, the meteorological conditions that trigger the fire are extremely seasonal. Meanwhile, the agriculture schedules are very stable in the eastern and northeast plains, and fires from *cropland only occur in and after the harvest seasons. For example the results shown in Fig.2, based on personal experience, I am very worried about the confusion of grassland and cropland fires.*

Response: Accepted. Seasonal patterns were introduced in Section 3.2. The spatial distributions of grassland and cropland fires shown in Fig.2 are reasonable. Grassland fires are mainly distributed in the mountains and hills in northeastern China and southern China. Cropland fires are concentrated in central China and northeastern China due to the burning of winter wheat residue in the North China Plain and corn straw in the Northeast China Plain.

Revisions: (Page 9, Line 17) "Seasonal variations of CO_2 emissions from each source were presented in Fig.4. In terms of total emissions, spring (March, April and May) contributed the most emissions due to the impact of dry weather. The lowest emissions occurred in rainy season including July, August, and September, producing 2.1,1.7, and 1.8 Tg CO_2, respectively. From the perspective of source-specific emissions, forest and grassland fires exhibited similar temporal variation, i.e., higher emissions in winter and spring, and lower emissions in summer. The highest emissions from forest and grassland fires occurred in the period of January to May. This pattern was strongly affected by favorable fire conditions such as low vegetation moisture content and high wind speed (Song et al., 2009). In addition, Li et al. (2015) found that a large portion of forest fires in spring were induced by sacrificial activity in Tomb-sweeping Day (April 5). Forest Fires in winter were concentrated in southern China due to the impacts of low precipitation and mild temperatures. In contrast, boreal forests rarely burned because of the low temperatures and moist snow cover. This result was consistent with the that reported by Chen et al. (2017a). The temporal distribution of shrubland fire emissions was also similar to that of forest and grassland fires, but emissions from bush only account for a small fraction of total levels (approximately 1 %). Emissions from crop burning were closely related to agriculture activities. Different main crops and sowing/harvest times in different areas lead to multiple emission peaks (Jin et al., 2018). Highest emissions occurred in summer, and small peaks were detected in spring and autumn. Emissions from agriculture fires contribute 84 % to total emissions in summer, which were concentrated in June due to the large amount of winter wheat straw burning in the North China Plain. From March to May, as large amounts of crop residues were burned to clear the cultivated land for sowing, fires were scattered throughout the country. In autumn (especially October), corn straws burning in the Northeast China Plain and late rice residue burning in southern China were primary contributors, and small areas of maize residue burning could be found in northern China (Chen et al., 2017a). During winter, crop burning mostly occurred in southern China due to citrus harvest and orchard clearing activity.”

3. Monte Carlo
Please explain more details in the Monte Carlo simulations, which (how many) independent variables are fitted and randomly sampled.

Response: Accepted. More details could be found in Section 4.

Revisions: (Page 12, Line 6) “In this study, we considered errors of three independent variables, namely FRE, conversion ratio and emission factors. According to the error budget suggested by Vermote et al. (2009), we assumed that the relative error of FRE and the conversion ratio was 31 % and 10 %, respectively. The uncertainty of the emission factor is species dependent and we applied the uncertainty suggested in Huang et al. (2012), as shown in Table S2. We ran 20,000 Monte Carlo simulations to estimate the range of average annual fire emissions in 2003–2017 with a 90 % confidence interval. In Monte Carlo simulation, random number were selected from normal distribution of input variables.”

4. Double check the words, including CO2 (2 subscript). Use “dry season” rather than “arid season”, different meanings.

Response: Accepted.

Revisions: (Page 1, Line 21) “Forest and grassland fires are concentrated in northeast and south China, especially in dry season (from October to March of the following year).”

Referee comment #2:

Review comment: reject. This study developed a biomass burning emission inventory for China from 2003 to 2017 using a method based on FRE and presented the change of biomass burning emissions from different land cover types. The reason for rejection is that the biomass burning emissions from different land cover types are not reasonable. The aim of this study is to construct an inventory of biomass burning emission for China that could be used in global and regional air quality modeling. So the accuracy of the emission data is very important for data users. In addition, the improving estimation of biomass burning emissions in this study over other estimations was not well proved. The main problem is that the land cover data used in the study is of low accuracy over China. Emission factors for each land-cover type were derived from published studies. So the emissions of different gases were related with land cover types. The quality of the land cover data decided the quality of the emission estimation. If the land cover data were not accurate, the results wouldn't be credible. However, all of the discussions were based on the inventory. The spatial distribution of CO2 emissions is not reasonable, especially the distribution from grassland, cropland, and shrublands. If you have read the papers about Chinese land cover written by Zengxiang Zhang et al (2014) and Jun Chen et al., (2016), you could find out that the distribution of the three land cover types were different from what the paper showed. I suggest that you could change the land cover data and improve your writing.

Response: We appreciate the review's comments, which indeed help us to improve the manuscript much. As the reviewer suggested, we used GlobeLand30 datasets instead of GlobCover 2009 in revised manuscript. GlobeLand30 maps global land cover at 30 m spatial resolution in two base years (2000 and 2010). In this study, the land cover types are characterized by GlobeLand30-2000 for years 2003–2005 and GlobeLand30-2010 for years 2006–2017. We wish you know that the NLUD-C (Zengxiang Zhang et al., 2014) is commercial at present, and the price is more than 80 thousand U.S. dollars for three years. We cannot afford them.

Some detailed comments and suggestions are listed as follows: The introduction didn't have a good logic. The aim of the study is to develop a biomass burning emission inventory for China from 2003 to 2017. The method based on FRE was not innovated by this study, but most of the introduction was about the most often used methods and approach based on FRE. In the introduction, the paper didn't provide a summary about the existing studies for Chinese biomass burning. Maybe some studies were mentioned when the method based on FRE was introduced. Although you mentioned that "few studies have used this approach to estimate emissions from agricultural burning on a national scale", the words didn't support this conclusion. What about other land cover types? What about regional scale? What's more, the cropland distributed intensively in several plains in China. It is not necessary to estimate emissions on a national scale if there are already some studies focusing on the main agricultural regions. Actually, the paper also studied other land cover types. Agricultural burning was not the only study *aim.*

Response: Accepted. We reworded the Introduction section according to your comments.

Revisions: (Page 2, Line 10) "Early studies used provincial statistical data to estimate biomass burning emissions. This method required many parameters that depend on local environment or agricultural practices and could vary greatly in different research, leading to significant emission uncertainties (Liu et al., 2015). Studies statistically evaluated fire emissions in China with results of annual CO_2 emissions of 68–150 Tg from crop residue burning (Ni et al., 2015; Huang et al., 2012; Li et al., 2016b) and 3–40 Tg from forest fires (Lu et al., 2006; Yan et al., 2006). This approach produced emission estimates at a coarse resolution that cannot be used for detailed analysis of spatiotemporal patterns. Thus, two methods based on remote sensing data has been increasingly used. The first one is based on fire count data provided by active fire products. In this approach, a maximum burned area of 1 km^2 is assumed for each fire count detected. Mehmood et al. (2018) calculated the mean emission of CO_2 for the period of 2002–2016 as 160 Tg yr^{-1} (with 24 Tg from crop residue burning) by using data derived from the Fire INventory from NCAR version 1.5 (FINNv1.5), which was established by the fire count method (Wiedinmyer et al., 2011). Because the actual area burned of each fire count could vary to a large extent, using fire counts as a proxy for fire-affected area may lead to great potential error on emission estimates (Song et al., 2009). The other one is based on the burned areas products (Song et al., 2010). The estimated emission is a product of burned area (km^2), aboveground biomass density burned in fields (kg dry matter m^{-2}), combustion efficiency (%), and emission factor (g kg^{-1}) for each pollutant. Generally, the uncertainty originates from all of the above factors. Moreover, as the average cultivated area of a farming household is very limited in China (around 10^4 m^2), each agricultural fire burns within a small extent (Liu et al., 2015). Therefore, the fire count method is likely to overestimate the burned area of crop residue burning, and these fires are not detected efficiently by the available burned area algorithms due to the small areas and intermittency (Song et al., 2009)."

(Page 3, Line 9) "The FRE method estimates biomass consumed according to energy radiated from fires, which could avoid the uncertainty caused by inaccuracy of satellite-derived burned area and therefore improve the estimation, especially for small fire emissions. Moreover, the amount of pollutants released by biomass burning could be calculated as a product of FRE, conversion ratio and emission factors, reducing uncertainties from multiple parameters that are not reliably defined at regional and global scales

(Wooster et al., 2005). Liu et al. (2015) applied FRE approach to estimate emissions of crop residue burning in North China Plain during the harvest season (June). The differences of their results with those derived from official statistic data (Huang et al., 2012) were mostly around −13 % with the largest difference of −49 %. Besides, their results were significantly higher than those derived from burned area product (MCD45A1). These comparisons suggested that the approach produced a reasonable estimation."

(Page 3, Line 23) "Some studies have used FRE method to estimate global and regional biomass burning emissions (Vadrevu et al., 2011; McCarty et al., 2012; Vermote et al., 2009). However, to our knowledge, few studies in China used this approach to estimate emissions from crop residue burning and other vegetation fires on a national scale. Thus, the establishment of a biomass burning emission inventory based on FRE method for the whole country is of great significance."

Page 1: line 10: what does "available emission factors" mean specifically?

Response: The emission factors we used in this study were cited from references listed in Supplement (Table S1).

Revisions: (Supplement, Table S1) "Note: Superscript letters indicate the data source: [a](Andreae and Merlet, 2001;Streets et al., 2003;Cao et al., 2004;Michel et al., 2005;Wiedinmyer et al., 2006). [b](Andreae and Merlet, 2001;Streets et al., 2001;Reddy and Venkataraman, 2002;Cao et al., 2006)."

Page 1: line 12: The paper didn't show how the method based on FRE provides a more reasonable estimate from small fires directly.

Response: Accepted. Detailed information had been added in Introduction section.

Revisions: (Page 3, Line 1) "… as the average cultivated area of a farming household is very limited in China (around 10^4 m^2), each agricultural fire burns within a small extent (Liu et al., 2015). Therefore, the fire count method is likely to overestimate the burned area of crop residue burning, and these fires are not detected efficiently by the available burned area algorithms due to the small areas and intermittency (Song et al., 2009)."

(Page 3, Line 9) "The FRE method estimates biomass burned amount according to energy radiated from fires, which could avoid the uncertainty caused by inaccuracy of satellite-derived burned area and therefore improve the estimation, especially for small fire emissions. Moreover, the amount of pollutants released by biomass burning could be calculated as a product of FRE, conversion ratio and emission factors, reducing uncertainties from multiple parameters that are not reliably defined at regional and global scales (Wooster et al., 2005)."

Page 1: line 19-21: this conclusion is not special for this study, so you don't have to put it here.

Response: Accepted. We improved the expression of our conclusion.

Revisions: (Page 1, Line 21) "Forest and grassland fires are concentrated in northeastern China and southern China, especially in dry season (from October to March of the following year). Plain areas with high crop yields, such as the North China Plain, experienced high agricultural fire emissions in harvest seasons. Most shrubland fires located in Yunnan and Guangdong province."

Page 2: line 7: a reference or link need to be added here. I doubted that biomass burning from crop residues leading to substantial pollutant emissions in China. The paper concluded that forest was the major source of biomass burning in China.

Response: Accepted. We added a reference here (Streets et al., 2003). In the revised manuscript, GlobeLand30 was used to characterize biomass type and the results still showed that forest fires contribute most to the total emissions. Actually, annual mean emissions from forest fires and crop residue burning are very closed (40.8 and 35.3 Tg CO_2, respectively). Most studies tend to focus on the emissions in eastern China and central China or densely populated regions to investigate the impacts of pollutants on human health. Crop residue burning extensively occurred in these areas due to the developed agriculture. In our study, agricultural fires are also determined to be the primary contributor in northeastern and central regions, accounting for 55 % of the total CO_2 emissions. However, forest fires are concentrated in north and southwest provinces, which are remote and sparsely populated. According to Yan et al. (2006), forest fires are substantially understated in official statistical data. Due to the high biomass density, forest fires would release large quantities of pollutants. Studies based on satellite burned area products reported that annual CO_2 emissions range from 19 to 137 Tg (Qiu et al., 2016;Song et al., 2009), which could account for a large portion of total biomass burning emission. Emissions caused by forest fires has not been studied in great detail.

Revisions: (Page 2, Line 9) "In China, the annual amount of crop residue burned in fields estimated by Streets et al. (2003) was 110 Tg, accounting for 44 % of all crop residue burned in Asia, leading to substantial pollutant emissions."

(Page 7, Line 12) "On a national scale, forest fires contribute the largest portion (45 %) of total CO_2 emissions from open fires. Agricultural fires and grassland fires ranked for the second and third places, accounting for 39 % and 15 %, respectively. Regionally, the main emission contributor is different. In southwestern region, the percentage of emission from forest fires could reach up to about 65 %, whereas the most important source in northeastern China is crop residue burning, accounting for 47 % of total emissions. The result was in connection with rural population intensity and land use patterns (Qiu et al., 2016). For example, due to the dense boreal forests and developed agriculture, the highest emission was found in Heilongjiang with 46 % from agriculture fires and 54 % from forest and grassland fires. Similarly, in the southwestern region, the dense vegetative cover of Yunnan-Guizhou Plateau greatly contributes to fire events. Benefiting from fertile land and favorable climate, northern and central regions contain many principal agricultural provinces (including Shandong, Henan, Hubei and Anhui Provinces) and therefore large amounts of crop residue were burned in field during the harvest season, contributing 55 % to the total emissions."

Page 3: line 12: to prove a method to be valid should base on field survey, not a comparison with results from another research.

Response: Accepted. Results of Huang et al. (2012) were based on statistical data, and we reworded the sentence.

Revisions: (Page 3, Line 13) "Liu et al. (2015) applied FRE approach to estimate emissions of crop residue burning in North China Plain during the harvest season (June). The differences of their results with those derived from official statistical data (Huang et al., 2012) were mostly around −13 % with the largest difference of −49 %. Besides, their results were significantly higher than those derived from burned area method. These comparisons suggested that the approach produced a reasonable estimation."

Page 3: line 12: it will be better to put "According to the accumulated temperature, China is. . ." into a new paragraph.

Response: Accepted.

Page 3: line 15: is the method that parameterizes the FRP diurnal cycle for crop zones and harvest seasons innovated by you, or it was proposed by former studies? If it was proposed by you, you should put it in the method section. If it was proposed by former study, a reference should be provided.

Response: Accepted. Detailed information had been added in Section 2.1.

Revisions: (Page 5, Line 18) "Different combustion characteristics of fuel types could be reflected by specific T/A ratio. As shown in Fig.S1 (excluding small islands in South China Sea), China is divided into six temperature zones (tropical zone, subtropical zone, warm-/middle-/cold–temperate zone and Qinghai-Tibet plateau). Because the dominate crop types vary greatly among temperature zones, we calculated T/A ratio for each zone separately. Using respective T/A ratio to calculate factors required in Eq. (2), the FRP diurnal cycle was parameterized for each zone and harvest season, which could reflect specific combustion characteristic of different straw types."

Page 3: line 23: introduction about the global land cover data should be put in the data section.

Response: Accepted.

Revisions: (Page 6, Line 9) "The GlobeLand30 dataset maps global land cover at 30 m spatial resolution in two base years (2000 and 2010) (Chen et al., 2017b), as shown in Fig S2 (small islands in the South China Sea are not included). GlobeLand30 data are generated by multispectral images derived from Landsat TM, ETM+ and Chinese Environmental Disaster Alleviation Satellite (HJ-1). The result of accuracy assessment shows that the overall accuracy of GlobeLand30 reaches 83.5 %. GlobeLand30 dataset consists of 10 land cover types, namely cultivated land, forest, grassland, shrubland, wetland, water bodies, tundra, artificial surfaces, bareland, permanent snow and ice. In this study, the land cover types are characterized by GlobeLand30-2000 for years 2003–2005 and GlobeLand30-2010 for years 2006–2017. We combined the land-cover map of China and the latitude and longitude data of fire count in MOD14/MYD14 to determine the biomass fuel types. For instance, if a fire count locates in cropland area, it will be considered as a crop residue burning event."

Page 4: line 10-12: why did you use the average value, not one of them? When the two values were provided, didn't the researchers give suggestions about their applications? As the CR was very important in calculating the emissions, the value should be decided more carefully.

Response: The field experiment conducted by Wooster et al. (2005) tried to replicate conditions of dry season savanna fires. The fuels used were Miscanthus, dried grasses, wheat stems and a woody fuel. The experiment of Freeborn et al. (2008) was conducted in combustion chamber, and most of the fuels used are wood and herbaceous. When Vermote et al. (2009) developed the modified Gaussian function to calculate FRE and estimate global biomass burning emissions, they applied the average of conversion factors from above two studies. We adopted the mean value for calculation referred to method of Vermote et al. (2009). The potential error of conversion factor had been considered in Monte Carlo simulations.

Revisions: (Page 12, Line 7) "According to the error budget suggested by Vermote et al. (2009), we assumed that the relative error of FRE and the conversion ratio was 31 % and 10 %, respectively."

Page 4: line 16: the method section should introduce the method used in the study and how you used the method to get the results, not the method provided by the former *research. The expression should be improved.*

Response: Accepted. We improved the expression as you suggested.

Revisions: (Page 4, Line 10) "Pollutant emissions were calculated as the product of dry mass burned (kg) and a corresponding emission factor (g kg^{-1}). In this study, emission factors for each land cover type were obtained from previous publications (Table S1). If more than one value for an emission factor is available, the average value is used. The amount of biomass consumed was calculated by multiplying FRE by a conversion ratio, which was not significantly influenced by vegetation types"

(Page 4, Line 20) "FRE was estimated by integrating FRP (i.e. instantaneous FRE) over the duration of the fire process. In this study, FRP data from MODIS active fire products (MOD14/MYD14) were used. The MODIS sensors, onboard the polar-orbiting satellites Terra and Aqua, acquire four discrete FRP data at 1030/2230 (Terra) and 0130/1330 (Aqua), equatorial local time. Therefore, the fire diurnal variation cannot be directly detected by satellite observation and many fire events have been missed. To calculate FRE and make up the omission error, we used a modified Gaussian function (Vermote et al., 2009) to parameterize the FRP diurnal cycle. This parameterization describes the discrete observations as a continuous function and simplifies integral process to calculate total fire energy released."

Page 4: line 24: that "the origin formula couldn't provide reasonable estimations" and that "h has little effect on the final calculation" seems to be contradictory.

Response: Accepted. We reworded the sentences.

Revisions: (Page 5, Line 13) "We found that the original parameterized FRP diurnal cycle could not agree well with the observed FRP temporal variation in China, possibly due to inaccurate FRP peak hour. Because it has been pointed that h has little effect on the final result of FRE (Vermote et al., 2009), we added a parameter ε (ε=4) in order to modify FRP peak hour (Liu et al., 2015)."

Page 5: line 2: is ε a constant or variable? Maybe a variable, as you didn't present its value. If it was a variable, how did you decide its value?

Response: Accepted.

Revisions: (Page 5, Line 14) "Because it has been pointed that h has little effect on the final result of FRE (Vermote et al., 2009), we added a parameter ε (ε=4) in order to modify FRP peak hour (Liu et al., 2015)."

Page 5: line 14: the expression is not accurate. GlobCover maybe the most detailed map of earth land surface at the same spatial resolution. The reference was not the newest. Many new land cover datasets have been produced in recent decades. Maybe other land cover datasets like Globeland30 (Jun Chen et al., 2016) or NLUD-C (Zengxiang Zhang et al., 2014) are more suitable. The four main land cover types used *in this study could be found in this dataset. And the accuracy of Globeland30 is better than GLobCover 2009 since it has higher spatial resolution.*

Response: Accepted. As you suggested, we used GlobeLand30 datasets instead of GlobCover 2009 in revised manuscript. GlobeLand30 maps global land cover at 30 m spatial resolution in two base years (2000 and 2010). In this study, the land cover types are characterized by GlobeLand30-2000 for years 2003–2005 and GlobeLand30-2010 for years 2006–2017.

Page 7: line 7: if figure 2 was presented on a national province map, it would be clearer that how the emissions distribute in different provinces. A land cover map can be presented simultaneously.

Response: Accepted. We presented Figure 2 on provincial level. The land cover map was presented in Figure S2. It is difficult to present them in one figure simultaneously as land cover map would be overlaid by emission distribution map.

20. Page 9: line 16: to decide if the results are reasonable or not, you should compare the calculating results with field data or the statistical data from government, not just compare it with other research data.

Response: Accepted. Comparisons of our results with those obtained from statistical data were shown in Section 3.2 and Section 3.3.

Revisions: (Page 8, Line 17) "Peak emissions occurred in 2003, 2009 and 2014; forest fires in 2003 and 2009, and cropland fires in 2014 were determined to be the primary contributors, accounting for 61 %, 56 %, and 49 % of total emissions in that year, respectively. Our results were in accordance with the records reported in official statistics. According to the China Forestry Statistical Yearbook, there are seven extraordinarily serious fire accidents in 2003, resulting in the largest forest burned area during the study period. A total of 35 serious fire accidents happened in 2009, 171 % higher than the 15-year average number of that kind of fire events (12.9)."

(Page 9, Line 1) "Pollutants released by crop straw burning continue to rise in 2003–2014, leading to a peak emission of 57.6 Tg CO_2 in 2014. Because crop residues burning in field could be well controlled by strict supervision, cropland emissions have decreased rapidly in 2015–2016 (dropped by 42 %). However, the emissions increased again by 37 % in 2017. This variation trend was similar to that concluded by studies based on statistical data (Li et al., 2016b; Jian et al., 2018). Yan et al. (2006) pointed that as the socioeconomic development, which results in a decline of biofuel (crop residue, fuel wood) demand, crop residue is increasingly being burned in the field. Tao et al. (2018) found that the consumption of crop residues as residential energy in rural China decreased by 51 % from 1992 to 2012. We noted that the number of agricultural fire count increased by a factor of 3 in 2003–2014 (from 13683 to 67143), which could support the conclusion as well. Although the controlling of pollutants from crop residue burning in China started from 1965, it seems to be ineffective and the crop straw burning should be further focused."

(Page 10, Line 20) "When compared with results of Huang et al. (2012) and Yan et al. (2006), which were based on official statistical data, our results were larger for forest and grassland fires, and underestimated for crop residue burning. According to Yan et al. (2006), forest and grassland fires were understated in statistics for both personal and political reasons. They suggested that satellite data are preferable to statistical data to estimate emissions from forest and grassland fires. When statistics were used to estimate crop residue emission, the crop residue burnt are calculated as a product of crop production, residue-to-production ratio, dry matter-to-crop residue ratio, the percentage of dry matter burned in fields, and combustion efficiency. Values of these parameters depend on local agricultural practices and vary greatly in different studies. For example, the value of percentage of residue burned in field, which is one of the most important factors to be determined, ranges from 6.6 % to 82 % in different research (Gao et al., 2002; Yang et al., 2008; Yan et al., 2006). The accumulation of uncertainties derived from multiple factors could result in significant emission uncertainties. Using statistical data, amount of burned residue was estimated to be 40–160 Tg yr^{-1}, showing a great potential error (Li et al., 2016a; Huang et al., 2012). Therefore, results derived from statistical are not necessarily reliable."

Page 9: line 18: if you mean that the discrepancy between the former studies (GFED4s and GFASv1) and your results is caused by the high omission rate of small fires in the two existing datasets, then you should prove this by comparing the two results directly, not just by citing a reference.

Response: Our results were closed to those derived from GFED4s and GFASv1, but substantially higher than those based on the burned area product (MCD64A1). As the FRE method calculate emissions based on radiated energy from fires, burned area data cannot be obtained from FRE method. It is difficult to compare the burned area data from two methods directly. However, when used data in MCD64A1 to make estimate, the burned area is the most important factor in determining fire emissions. Therefore, the underestimation in results from MCD64A1 can primarily attribute to the high omission rate of small fires and uncertainty in the calculation of fire-affected area.

Revisions: (Page 10, Line 15) "… as shown in Table 3, results calculated by using data from burned area product MCD64A1 were substantially underestimated. In this method, burned area is one of the most important factors in calculating emissions, so that the underestimation could be attributed to omission of fires with small areas and short duration (Song et al., 2009)."

Page 10: line 10: although the paper concluded that the estimation of biomass burning emissions in this study was improved, it was hard to confirm its credibility. As the words "perhaps due to" were used in this paper.

Response: Accepted. We improved the expression. We concluded that our estimation was improved by the comparison of results based on FRE method with those based on statistical and satellite data.

Revisions: (Page 10, Line 20) "When compared with results of Huang et al. (2012) and Yan et al. (2006), which were based on official statistical data, our results were larger for forest and grassland fires, and underestimated for crop residue burning. According to Yan et al. (2006), forest and grassland fires were understated in statistics for both personal and political reasons. They suggested that satellite data are preferable to statistical data to estimate emissions from forest and grassland fires. When statistics were used to estimate crop residue emission, the crop residue burnt are calculated as a product of crop production, residue-to-production ratio, dry matter-to-crop residue ratio, the percentage of dry matter burned in fields, and combustion efficiency. Values of these parameters depend on local agricultural practices and vary greatly in different studies. For example, the value of percentage of residue burned in field, which is one of the most important factors to be determined, ranges from 6.6 % to 82 % in different research (Gao et al., 2002; Yang et al., 2008; Yan et al., 2006). The accumulation of uncertainties derived from multiple factors could result in significant emission uncertainties. Using statistical data, amount of burned residue was estimated to be 40–160 Tg yr^{-1}, showing a great potential error (Li et al., 2016a; Huang et al., 2012). Therefore, results derived from statistical are not necessarily reliable. When compared to other inventories based on remote sensing data, our results agreed well with those reported by GFED4s and were substantially higher than those derived from burned area product (MCD64A1). Datasets in GFED4s are based on burned area boosted by small fire burned area, which could provide a relatively high emission estimation of agricultural fires."

(Page 11, Line 18) "Our results were higher than those based on burned area products as the FRE method avoids uncertainties cause by inaccuracy of satellite-derived burned area and multiple other parameters. The results were closed to those derived from FINNv1.5 in terms of emissions from grassland and cropland fires and accorded with those from GFED4s for all fire types. The temporal and spatial resolution of our inventory (daily, 1 km) are higher than that of GFED4s (monthly, 0.25 degrees) and GFASv1.0 (daily, 0.5

degrees). Compared with other inventories, we considered specific combustion characteristics of different crop types and calculated the agriculture fires emissions separately according to the distribution of temperate zones. Therefore, this method developed a high-resolution inventory and improved estimation of biomass burning emissions, especially for small fires in cropland."

Page 10: line 20: in this paragraph, you mentioned several sources of errors. The Monte Carlo simulations seemed to calculate the uncertainty caused by emission factors. What about the uncertainties caused by other error sources?

Response: Uncertainties of three independent variables are considered in Monte Carlo simulations, namely FRE, conversion ratio and emission factors. More details could be found in Section 4.

Revisions: (Page 12, Line 6) "In this study, we considered errors of three independent variables, including FRE, conversion ratio and emission factors. According to the error budget suggested by Vermote et al. (2009), we assumed that the relative error of FRE and the conversion ratio was 31 % and 10 %, respectively. The uncertainty of the emission factor is species dependent and we applied the uncertainty suggested in Huang et al. (2012), as shown in Table S2. We ran 20,000 Monte Carlo simulations to estimate the range of average annual fire emissions in 2003–2017 with a 90 % confidence interval. In Monte Carlo simulation, random number were selected from normal distribution of input variables."

Page 11: line 13: if your estimates were just very close to the results from GFED4s and GFASv1.0, then why the users would choose your estimations?

Response: Considering different combustion characteristics of different crop types, the agriculture fires emissions are calculated separately according to the distribution of temperate zones in our method. Besides, the temporal and spatial resolution of our inventory (daily, 1 km) are higher than that of GFED4s (monthly, 0.25 degrees) and GFASv1.0 (daily, 0.5 degrees).

Revisions: (Page 11, Line 19) "The results were closed to those derived from FINNv1.5 in terms of emissions from grassland and cropland fires and accorded with those from GFED4s for all fire types. The temporal and spatial resolution of our inventory (daily, 1 km) are higher than that of GFED4s (monthly, 0.25 degrees) and GFASv1.0 (daily, 0.5 degrees). Compared with other inventories, we considered specific combustion characteristics of different crop types and calculated the agriculture fires emissions separately according to the distribution of temperate zones. Therefore, this method developed a high-resolution inventory and improved estimation of biomass burning emissions, especially for small fires in cropland."

References:

Freeborn, P. H., Wooster, M. J., Hao, W. M., Ryan, C. A., Nordgren, B. L., Baker, S. P., and Ichoku, C.: Relationships between energy release, fuel mass loss, and trace gas and aerosol emissions during laboratory biomass fires, Journal of Geophysical Research, 113, 10.1029/2007jd008679, 2008.

Huang, X., Li, M., Li, J., and Song, Y.: A high-resolution emission inventory of crop burning in fields in China based on MODIS Thermal Anomalies/Fire products, Atmospheric Environment, 50, 9-15, 10.1016/j.atmosenv.2012.01.017, 2012.

Qiu, X., Duan, L., Chai, F., Wang, S., Yu, Q., and Wang, S.: Deriving High-Resolution Emission Inventory of Open Biomass Burning in China based on Satellite Observations, Environ Sci Technol, 50, 11779-11786, 10.1021/acs.est.6b02705, 2016.

Song, Y., Liu, B., Miao, W., Chang, D., and Zhang, Y.: Spatiotemporal variation in nonagricultural open fire emissions in China from 2000 to 2007, Global biogeochemical cycles, 23, 2009.

Streets, D., Yarber, K., Woo, J. H., and Carmichael, G.: Biomass burning in Asia: Annual and seasonal estimates and atmospheric emissions, Global Biogeochemical Cycles, 17, 2003.

Vermote, E., Ellicott, E., Dubovik, O., Lapyonok, T., Chin, M., Giglio, L., and Roberts, G. J.: An approach to estimate global biomass burning emissions of organic and black carbon from MODIS fire radiative power, Journal of Geophysical Research, 114, 10.1029/2008jd011188, 2009.

Wooster, M. J., Roberts, G., Perry, G. L. W., and Kaufman, Y. J.: Retrieval of biomass combustion rates and totals from fire radiative power observations: FRP derivation and calibration relationships between biomass consumption and fire radiative energy release, Journal of Geophysical Research, 110, 10.1029/2005jd006318, 2005.

Yan, X., Ohara, T., and Akimoto, H.: Bottom-up estimate of biomass burning in mainland China, Atmospheric Environment, 40, 5262-5273, 10.1016/j.atmosenv.2006.04.040, 2006.

Estimation of emissions from biomass burning in China (2003–2017) based on MODIS fire radiative energy data

Lifei Yin[1], Pin Du[1], Minsi Zhang[2], Mingxu Liu[1], Tingting Xu[1], Yu Song[1]

[1]State Key Joint Laboratory of Environmental Simulation and Pollution Control, Department of Environmental Science, Peking University, Beijing, China

[2]National Center for Climate Change Strategy and International Cooperation (NCSC), Beijing, China

Correspondence to: Yu Song (songyu@pku.edu.cn)

Abstract. Biomass burning plays a significant role in air pollution and climate change. In this study, we used the method based on fire radiative energy (FRE) to develop a biomass burning emission inventory for China from 2003 to 2017. Daily fire radiative power (FRP) data derived from 1 km MODIS Thermal Anomalies/Fire products (MOD14/MYD14) were used to calculate FRE and combusted biomass. Available emission factors were assigned to four biomass burning types: forest, cropland, grassland and shrubland fires. The farming system and crop types in different temperate zones were taken into account in this research. Compared with traditional methods, the FRE method was found to provide a more reasonable estimates of emissions from small fires. The estimated average annual emission ranges, with a 90 % confidence interval, were 91.4 (72.7–108.8) Tg CO_2 yr^{-1}, 5.0 (2.3–7.8) Tg CO yr^{-1}, 0.24 (0.05–0.48) Tg CH_4 yr^{-1}, 1.43 (0.53–2.35) Tg NMHC yr^{-1}, 0.23 (0.05–0.45) Tg NO_x yr^{-1}, 0.09 (0.02–0.17) Tg NH_3 yr^{-1}, 0.03 (0.01–0.05) Tg SO_2 yr^{-1}, 0.04 (0.01–0.08) Tg BC yr^{-1}, 0.27 (0.07–0.49) Tg OC yr^{-1}, 0.51 (0.19–0.84) Tg $PM_{2.5}$ yr^{-1}, 0.57 (0.15–1.05) Tg PM_{10} yr^{-1}. Forest fires are determined to be the primary contributor to open fire emissions, accounting for 45 % of the total CO_2 emissions (average 40.8 Tg yr^{-1}). Crop residue burning ranked for the second places with a large portion of 39 % (average 35.3 Tg yr^{-1}). During the study period, emissions from forest and grassland fires showed a significant downward trend. Crop residue emissions continued to rise during 2003–2015 but dropped by 42 % in 2015–2016. Emissions from shrubland were negligible and little changed. Forest and grassland fires are concentrated in northeastern China and southern China, especially in dry season (from October to March of the following year). Plain areas with high crop yields, such as the North China Plain, experienced high agricultural fire emissions in harvest seasons. Most shrubland fires located in Yunnan and Guangdong province. The resolution of our inventory (daily, 1

km) is much higher than previous inventories, such as GFED4s and GFASv1.0. It could be used in global and regional air quality modeling.

1. Introduction

Biomass burning is an important source of gaseous and particulate matter emissions to the troposphere (Crutzen et al., 1979;Seiler and Crutzen, 1980). Globally, biomass burning contributes around 20 %–30 % of CO_2 emissions and chemically active gases such as hydrocarbons, CO and NO_x (Andreae, 1991), approximately 42 % of black carbon (BC), and 74 % of primary organic carbon (OC) (Bond et al., 2004). These compounds have significant impacts on air quality, atmospheric chemistry, climate change, and human health (Andreae et al., 1994;Reid et al., 2005).

In China, the annual amount of crop residue burned in fields estimated by Streets et al. (2003) was 110 Tg, accounting for 44 % of all crop residue burned in Asia, leading to substantial pollutant emissions. Emission from other types of biomass burning, such as forest fires, are also of great concern (Chen et al., 2017a). Early studies used provincial statistical data to estimate biomass burning emissions. This method required many parameters that depend on local environment or agricultural practices and could vary greatly in different research, leading to significant emission uncertainties (Liu et al., 2015). Studies statistically evaluated fire emissions in China with results of annual CO_2 emissions of 68–150 Tg from crop residue burning (Ni et al., 2015;Huang et al., 2012;Li et al., 2016b) and 3–40 Tg from forest fires (Lu et al., 2006;Yan et al., 2006). This approach produced emission estimates at a coarse resolution that cannot be used for detailed analysis of spatiotemporal patterns. Thus, two methods based on remote sensing data has been increasingly used. The first one is based on fire count data provided by active fire products. In this approach, a maximum burned area of 1 km^2 is assumed for each fire count detected. Mehmood et al. (2018) calculated the mean emission of CO_2 for the period of 2002–2016 as 160 Tg yr^{-1} (with 24 Tg from crop residue burning) by using data derived from the Fire INventory from NCAR version 1.5 (FINNv1.5), which was established by the fire count method (Wiedinmyer et al., 2011). Because the actual area burned of each fire count could vary to a large extent, using fire counts as a proxy for fire-affected area may lead to great potential error on emission estimates (Song et al., 2009). The other one is based on the burned areas products (Song et al., 2010). The estimated emission is a product of burned area (km^2), aboveground biomass density burned in fields (kg dry matter m^{-2}), combustion efficiency (%), and emission factor (g

kg^{-1}) for each pollutant. Generally, the uncertainty originates from all of the above factors. Moreover, as the average cultivated area of a farming household is very limited in China (around 10^4 m^2), each agricultural fire burns within a small extent (Liu et al., 2015). Therefore, the fire count method is likely to overestimate the burned area of crop residue burning, and these fires are not detected efficiently by the available burned area algorithms due to the small areas and intermittency (Song et al., 2009). For a better estimation of biomass burning emission, an approach based on fire radiative energy (FRE) was proposed as a new tool for global studies of vegetation fires around the year 2000 (Kaufman et al., 1996;Wooster, 2002). FRE is the amount of energy radiated during the combustion process (Kaufman et al., 1996). The fuel mass consumed could be calculated by multiplying FRE by a conversion ratio, which has been demonstrated to be insensitive to vegetation type and could be treated as a constant (Freeborn et al., 2008;Wooster, 2002). The FRE method estimates biomass consumed according to energy radiated from fires, which could avoid the uncertainty caused by inaccuracy of satellite-derived burned area and therefore improve the estimation, especially for small fire emissions. Moreover, the amount of pollutants released by biomass burning could be calculated as a product of FRE, conversion ratio and emission factors, reducing uncertainties from multiple parameters that are not reliably defined at regional and global scales (Wooster et al., 2005). Liu et al. (2015) applied FRE approach to estimate emissions of crop residue burning in North China Plain during the harvest season (June). The differences of their results with those based on official statistical data (Huang et al., 2012) were mostly around −13 % with the largest difference of −49 %. Besides, their results were significantly higher than those derived from burned area product (MCD45A1). These comparisons suggested that the approach produced a reasonable estimation.

According to the accumulated temperature, China is divided into six temperature zones (tropical zone, subtropical zone, warm-/middle-/cold–temperate zone and Qinghai-Tibet plateau) (Shi, 2015). The growth period and main crop type varies among temperature zones. For example, in tropical regions, the main crops are rice, sugarcane and natural rubber, and rice grown there could be harvested for three times per year. While in middle-temperate zone, the main crops are spring wheat, maize and soybean, which ripen only once a year. Liu et al. (2015) focused on emissions from winter wheat residue burning in June, the result of which is not suitable for the whole country. Some studies have used FRE method to estimate global and regional biomass burning emissions (Vadrevu et al., 2011;McCarty et al., 2012;Vermote et al., 2009). However, to our knowledge, few studies in China used this approach to estimate emissions from crop residue burning and other vegetation fires on a national scale. Thus, the establishment of a biomass burning emission inventory based on FRE method for the whole country is of great significance.

In this study, we used FRP data derived from the MODIS active fire products to calculate emissions of 11 pollutants from biomass burning in China (excluding fires occurring on the small islands in the South China Sea) for the period of 2003–2017. The spatiotemporal distribution of emissions from four biomass burning types (forest, grassland, cropland, and shrubland fires) were detailed studied. A daily gridded 1 km emission inventory of biomass burning was established; this inventory could meet the requirements of global and regional air quality simulations.

2. Methods and data

2.1 Methods

Pollutant emissions were calculated as the product of dry mass burned (kg) and a corresponding emission factor (g kg^{-1}). In this study, emission factors for each land cover type were obtained from previous publications (Table S1). If more than one value for an emission factor is available, the average value is used.

The amount of biomass consumed was calculated by multiplying FRE by a conversion ratio, which was not significantly influenced by vegetation types (Wooster et al., 2005):

$$M = FRE \times CR \qquad (1)$$

Where M is the dry biomass consumed of one grid cell, FRE is the total radiative energy during the fire lifespan for one grid cell, and CR is the conversion ratio (kg MJ^{-1}) used to convert FRE to combusted biomass.

Wooster et al. (2005) reported a conversion ratio of 0.368 ± 0.015 kg MJ^{-1}, and that evaluated by Freeborn et al. (2008) was 0.453 ± 0.068 kg MJ^{-1}. In this study, we used the average value (0.411 kg MJ^{-1}).

FRE was estimated by integrating FRP (i.e. instantaneous FRE) over the duration of the fire process. In this study, FRP data from MODIS active fire products (MOD14/MYD14) were used. The MODIS sensors, onboard the polar-orbiting satellites Terra and Aqua, acquire four discrete FRP data at 1030/2230 (Terra) and 0130/1330 (Aqua), equatorial local time. Therefore, the fire diurnal variation cannot be directly detected by satellite observation and many fire events have been missed. To calculate FRE and make up the omission error, we used a modified Gaussian function (Vermote et al., 2009) to parameterize the FRP diurnal cycle. This parameterization describes the discrete observations as a continuous function and simplifies integral process to calculate total fire energy released. The modified Gaussian function is:

$$FRE = \int FRP = \int_0^{24} FRP_{peak} (b + e^{-\frac{(t-h)^2}{2\sigma^2}})\, dt \tag{2}$$

Where FRP_{peak} represents the peak of the diurnal cycle, b represents the background FRP, σ represents the standard deviation of the curve, and h represents the hour of peak FRP.

Monthly mean Terra and Aqua FRP (T/A ratio) was used to determine the required parameters with following equations (Vermote et al., 2009) :

$$b = 0.86x^2 - 0.52x + 0.08 \tag{3}$$

$$\sigma = 3.89x + 1.03 \tag{4}$$

$$h = -1.23x + 14.57 \tag{5}$$

$$FRP_{peak} = \frac{FRP_{Aqua\ Day}}{[b + e^{-\frac{(13.5-h)^2}{2\sigma^2}}]} \tag{6}$$

Where x represents the T/A ratio. We found that the original parameterized FRP diurnal cycle could not agree well with the observed FRP temporal variation in China, possibly due to inaccurate FRP peak hour. Because it has been pointed that h has little effect on the final result of FRE (Vermote et al., 2009), we added a parameter ε ($\varepsilon=4$) in order to modify FRP peak hour (Liu et al., 2015). The modified equation was:

$$h = -1.23x + 14.57 + \varepsilon \tag{7}$$

Monthly mean T/A ratio were calculated for each type of biomass burning. Different combustion characteristics of fuel types could be reflected by specific T/A ratio. As shown in Fig.S1 (excluding small islands in South China Sea), China is divided into six temperature zones (tropical zone, subtropical zone, warm-/middle-/cold–temperate zone and Qinghai-Tibet plateau). Because the dominate crop types vary greatly among temperature zones, we calculated T/A ratio for each zone separately. Using respective T/A ratio to calculate factors required in Eq. (2), the FRP diurnal cycle was parameterized for each zone and harvest season, which could reflect specific combustion characteristic of different straw types.

2.2 Data

The MODIS Thermal Anomalies/Fire 5-Min L2 Swath Products (MOD14/MYD14) are primarily derived from MODIS 4- and 11-micrometer radiances. The products provide the fire occurrence, location, FRP and other information of fire events with moderate spatial resolution (1 km^2) and high temporal resolution (daily). MOD14 data were obtained from Terra, which passes at 10:30 and 22:30 local time (LT), and MYD14 data were provided by Aqua, which acquires observations at 01:30 and 13:30 (LT). If Terra and Aqua detected the same fire events (determined by the time and location of fire occurrence), we would use information from Aqua since there is almost no difference between Terra and Aqua data and choosing Aqua can support the FRP_{peak} calculation. We used data for a 15-year period (2003–2017) to calculate FRE and estimate emissions.

The GlobeLand30 dataset maps global land cover at 30 m spatial resolution in two base years (2000 and 2010) (Chen et al., 2017b), as shown in Fig S2 (small islands in the South China Sea are not included). GlobeLand30 data are generated by multispectral images derived from Landsat TM, ETM+ and Chinese Environmental Disaster Alleviation Satellite (HJ-1). The result of accuracy assessment shows that the overall accuracy of GlobeLand30 reaches 83.5 %. GlobeLand30 dataset consists of 10 land cover types, namely cultivated land, forest, grassland, shrubland, wetland, water bodies, tundra, artificial surfaces, bareland, permanent snow and ice. In this study, the land cover types are characterized by GlobeLand30-2000 for years 2003–2005 and GlobeLand30-2010 for years 2006–2017. We combined the land-cover map of China and the latitude and longitude data of fire count in MOD14/MYD14 to determine the biomass fuel types. For instance, if a fire count locates in cropland area, it will be considered as a crop residue burning event.

To compare the results, we computed open fire emissions using data derived from MODIS burned area products (MCD64A1, http://modis-fire.umd.edu/), the fourth version of the Global Fire Emission Database (with small fires) (GFED4s), Global Fire Assimilation System (GFASv1.0), and FINNv1.5 (http://bai.acom.ucar.edu/Data/fire/). We derived data for 2003–2017 from MCD64A1, which is a monthly, global gridded 500 m product containing per-pixel burned area information. GFED4s provides monthly emission data at a spatial resolution of 0.25°; the latest GFED4s data are for 2016. GFASv1.0 calculates daily biomass burning emissions by assimilating FRP data from MODIS sensors on a global 0.5°×0.5° grid; we used GFASv1.0 data to estimate emission from 2003 to 2013. FINNv1.5 provides daily high-resolution (1 km) emissions of global biomass burning; data from 2003 to 2016 were used for comparison in this study.

3. Results and discussion

A total of 462,525 biomass fire pixels were detected by Terra, and 492,822 by Aqua from 2003 to 2017. When a fire pixel was probed by both satellites within the same day, the Terra pixel was removed to avoid repeated computations. Thus, a total of 942,933 fire pixels were applied to estimate emissions. The inter-annual variation in emissions was shown in Table 1. For the 15-year study period, average emissions of CO_2, CO, CH_4, NMHC, NO_x, NH_3, SO_2, BC, OC, $PM_{2.5}$, and PM_{10} were estimated to be 91.4, 4.0, 0.24, 1.43, 0.23, 0.09, 0.03, 0.04, 0.27, 0.51 and 0.57 Tg yr^{-1}, respectively. Taking CO_2 emission as an example, the maximum emission occurred in 2003 (123.0 Tg), followed by 2014 (117.3 Tg), and the minimum emission occurred in 2016 (59.8 Tg). These results will be discussed in detail in Section 3.2.

3.1 Spatial distribution of emissions

Average annual emissions of 11 pollutants at the provincial level were listed in Table 2, and source-specific emissions of CO_2 for each province were presented in Fig.1. Using CO_2 as a representative example, southwestern China and northeastern China contribute most to the total emission, with portion of 28 % and 26 %, respectively. On a national scale, forest fires contribute the largest portion (45 %) of total CO_2 emissions from open fires. Agricultural fires and grassland fires ranked for the second and third places, accounting for 39 % and 15 %, respectively. Regionally, the main emission contributor is different. In southwestern region, the percentage of emission from forest fires could reach up to 65 %, whereas the most important source in northeastern China is crop residue burning, accounting for 47 % of total emissions. The result was in connection with rural population intensity and land use patterns (Qiu et al., 2016). For example, due to the dense boreal forests and developed agriculture, the highest emission was found in Heilongjiang with 46 % from agriculture fires and 54 % from forest and grassland fires. Similarly, in the southwestern region, the dense vegetative cover of Yunnan-Guizhou Plateau greatly contributes to fire events. Benefiting from fertile land and favorable climate, northern and central regions contain many principal agricultural provinces (including Shandong, Henan, Hubei and Anhui Provinces) and therefore large amounts of crop residue were burned in field during the harvest season, contributing 55 % to the total emissions. Southeastern provinces in the Middle-Lower Yangtze River Plain and the southeastern hills have abundant cultivated land and forest resources, resulting in relatively high CO_2 emissions from cropland and forest fires (with portion of 32 % and 56 %, respectively). Northwestern

China experience extremely dry weather, which leads to low vegetative cover and negligible emissions from biomass burning. For instance, annual mean CO_2 released from open fires in Ningxia and Qinghai were 0.21 Tg and 0.13 Tg, respectively. Vegetation in these areas mainly consists of grass and a few drought-resistant crops; hence, an extremely high proportion (92 %) of CO_2 emissions in the northwest arose from grassland and cropland fires.

Nationwide spatial patterns of CO_2 emissions from four sources were shown in Fig. 2 (biomass fire emissions from the small islands in the South China Sea are not included). Forest and grassland fire emissions were mainly distributed in northeastern China and southern China. Dense vegetative covers in Yunnan-Guizhou Plateau, Inner Mongolian Plateau, Daxing'anling, Xiaoxing'anling and the southeast hills greatly contribute to fire events. Cropland fire emissions were concentrated in the three great plains of China, namely the Northeast China Plain, the North China Plain, and the Middle–Lower Yangtze Plain. Because of high crop production in these areas, large quantities of agricultural residues were burned in fields during the short period following the harvest season. In addition, due to snowmelt in the Tianshan Mountains, there are many oases located at the foot of the mountain range in Xinjiang Province. These oases are suitable for growing crops such as wheat and maize (Zhou et al., 2017). Therefore, crop fire emissions in Xinjiang province were higher than those in other northwestern provinces. Compared with other fire types, emissions from shrubland fire were negligible and the high emissions were concentrated in Guangdong and Yunnan province.

3.2 Temporal pattern of emissions

The annul variations of total and source–specific CO_2 emissions were presented in Fig.3. Peak emissions occurred in 2003, 2009 and 2014; forest fires in 2003 and 2009, and cropland fires in 2014 were determined to be the primary contributors, accounting for 61 %, 56 %, and 49 % of total emissions in that year, respectively. Our results were in accordance with the records reported in official statistics. According to the China Forestry Statistical Yearbook, there are seven extraordinarily serious fire accidents in 2003, resulting in the largest forest burned area during the study period. A total of 35 serious fire accidents happened in 2009, 171 % higher than the 15-year average number of that kind of fire events (12.9). As over 95 % of forest fires in China are caused by human activities, the implement of strict forest conservation policies and the development of fire control technology contribute significantly to the emission decline (Huang et al., 2011). Forest fires are well controlled after 2003 and emissions decreased by 78 % during the study period (from 74.7 Tg in 2003 to 16.6 Tg in 2017). Pollutants released by crop straw burning continue to rise in 2003–2014, leading to a peak emission of 57.6 Tg CO_2 in 2014. Because crop residues burning in field could be well controlled by strict supervision, cropland emissions have decreased rapidly in 2015–2016 (dropped by 42 %). However, the emissions increased again by 37 % in 2017. This variation trend was similar to that concluded by studies based on statistical data (Li et al., 2016b;Jian et al., 2018). Yan et al. (2006) pointed that as the socioeconomic development, which results in a decline of biofuel (crop residue, fuel wood) demand, crop residue is increasingly being burned in the field. Tao et al. (2018) found that the consumption of crop residues as residential energy in rural China decreased by 51 % from 1992 to 2012. We noted that the number of agricultural fire count increased by a factor of 3 in 2003–2014 (from 13683 to 67143), which could support the conclusion as well. Although the controlling of pollutants from crop residue burning in China started from 1965, it seems to be ineffective and the crop straw burning should be further focused. Emissions from grassland fires dropped by 60 % from 2003 to 2017 due to the conservation and supervision measures. Shrubland fire emissions were much lower than other fire emissions (range from 0.5 to 2.3 Tg yr^{-1}) and remained relatively stable during the study period. Emissions from forest, grassland and shrubland exhibited a small peak in 2014. According to the statistics, the total burned areas in 2014 for both forest and grassland are higher than previous years. The rise in burned area and emission could be attributed to an unusual warm condition occurred in 2014, which could facilitate the occurrence and spread of fires (Bond et al., 2015).

Seasonal variations of CO_2 emissions from each source were presented in Fig.4. In terms of total emissions, spring (March, April and May) contributed the most emissions due to the impact of dry weather. The lowest emissions occurred in rainy season including July, August, and September, producing 2.1,1.7, and 1.8 Tg CO_2, respectively. From the perspective of source-specific emissions, forest and grassland fires exhibited similar temporal variation, i.e., higher emissions in winter and spring, and lower emissions in summer. The highest emissions from forest and grassland fires occurred in the period of January to May. This pattern was strongly affected by favorable fire conditions such as low vegetation moisture content and high wind speed (Song et al., 2009). In addition, Li et al. (2015) found that a large portion of forest fires in spring were induced by sacrificial activity in Tomb-sweeping Day (April 5). Forest Fires in winter were concentrated in southern China due to the impacts of low precipitation and mild temperatures. In contrast, boreal forests rarely burned because of the low temperatures and moist snow cover. This result was consistent with the that reported by Chen et al. (2017a). The temporal distribution of shrubland fire emissions was also similar to that of forest and grassland fires, but emissions from bush only account for a small fraction of total levels (approximately 1 %). Emissions from crop burning were closely related to agriculture activities. Different main crops and sowing/harvest times in different areas lead to multiple emission peaks (Jin et al., 2018). Highest emissions occurred in summer, and small peaks were detected in spring and autumn. Emissions from agriculture fires contribute 84 % to total emissions in summer, which were concentrated in June due to the large amount of winter wheat straw burning in the North China Plain. From March to May, as large amounts of crop residues were burned to clear the cultivated land for sowing, fires were scattered throughout the country. In autumn (especially October), corn straws burning in the Northeast China Plain and late rice residue burning in southern China were primary contributors, and small areas of maize residue burning could be found in northern China (Chen et al., 2017a). During winter, crop burning mostly occurred in southern China due to citrus harvest and orchard clearing activity.

3.3 Comparison with other studies

The average annual emission estimates calculated in this study were compared to those based on data from the burned area product (MCD64A1), GFED4s, GFASv1.0, and FINNv1.5 (Table 3). Generally, our results were closed to those derived from GFED4s and GFASv1. However, as shown in Table 3, results calculated by using data from burned area product MCD64A1 were substantially underestimated. In this method, burned area is one of the most important factors in calculating emissions, so that the underestimation could be attributed to omission of fires with small areas and short duration (Song et al., 2009). Emission estimates by FINNv1.5 were higher than those of this study with a difference ranging from 29 % to 194 %.

The comparison of annual mean CO_2 emission from each fire type in our study with those derived from other methods was listed in Table 4 (shrubland and grassland fires are lumped into one category in GFED4s). When compared with results of Huang et al. (2012) and Yan et al. (2006), which were based on official statistical data, our results were larger for forest and grassland fires, and underestimated for crop residue burning. According to Yan et al. (2006), forest and grassland fires were understated in statistics for both personal and political reasons. They suggested that satellite data are preferable to statistical data to estimate emissions from forest and grassland fires. When statistics were used to estimate crop residue emission, the amount of crop residue consumed are calculated as a product of crop production, residue-to-production ratio, dry matter-to-crop residue ratio, the percentage of dry matter burned in fields, and combustion efficiency. Values of these parameters depend on local agricultural practices and vary greatly in different studies. For example, the value of percentage of residue burned in field, which is one of the most important factors to be determined, ranges from 6.6 % to 82 % in different research (Gao et al., 2002;Yang et al., 2008;Yan et al., 2006). The accumulation of uncertainties derived from multiple factors could result in significant emission uncertainties. Using statistical data, amount of burned residue was estimated to be 40–160 Tg yr^{-1}, showing a great potential error (Li et al., 2016a;Huang et al., 2012). Therefore, results derived from statistical are not necessarily reliable. When compared to other inventories based on remote sensing data, our results agreed well with those reported by GFED4s and were substantially higher than those derived from burned area product (MCD64A1). Datasets in GFED4s are based on burned area boosted by small fire burned area, which could provide a relatively high emission estimation of agricultural fires. Due to shielding by the dense canopy (Moreira de Araújo et al., 2012;Roy and Boschetti, 2009) and higher small-fire omission rates, emissions derived from burned area product (MCD64A1) were underestimated by 33 % -93 %, especially for forest fire (−85 %) and cropland fire (−93 %) emissions. FINNv1.5 emission estimates were higher for forest and shrubland fires. The discrepancy can primarily be attributed to the overestimation of burned area of forest fires (Roy et al., 2008) and different land cover characterization maps used. Estimates of grassland and cropland fire emissions in FINNv1.5 were closed to our results, with differences of 3 % and 8 %, respectively.

In conclusion, our estimates were higher than those based on statistics for forest and grassland fire emissions, but lower for crop residue burning emission. Our results were higher than those based on burned area products as the FRE method avoids uncertainties cause by inaccuracy of satellite-derived burned area and multiple other parameters. The results were closed to those derived from FINNv1.5 in terms of emissions from grassland and cropland fires and accorded with those from GFED4s for all fire types. The temporal and spatial resolution of our inventory (daily, 1 km) are higher than that of GFED4s (monthly, 0.25 degrees) and GFASv1.0 (daily, 0.5 degrees). Compared with other inventories, we considered specific combustion characteristics of different crop types and calculated the agriculture fires emissions separately according to the distribution of temperate zones. Therefore, this method developed a high-resolution inventory and improved estimation of biomass burning emissions, especially for small fires in cropland.

4 Uncertainty

Several sources of error impact the accuracy of our estimate. The first error source is related to the radiative energy diurnal cycle parameterization that impacts the calculation of FRE. In addition, the error in the fire detection and empirical formula for computing FRP have a considerable impact on the accuracy of FRE. The use of the conversion ratio in order to convert FRE to combusted biomass is one of error sources as well. Since emission factors vary in time and space, they could also bring large uncertainties. In this study, we considered errors of three independent variables, namely FRE, conversion ratio and emission factors. According to the error budget suggested by Vermote et al. (2009), we assumed that the relative error of FRE and the conversion ratio was 31 % and 10 %, respectively. The uncertainty of the emission factor is species dependent and we applied the uncertainty suggested in Huang et al. (2012) , as shown in Table S2. We ran 20,000 Monte Carlo simulations to estimate the range of average annual fire emissions in 2003–2017 with a 90 % confidence interval. In Monte Carlo simulation, random number were selected from normal distribution of input variables. Estimated emissions of CO_2, CO, CH_4, NMHC, NO_x, NH_3, SO_2, BC, OC, $PM_{2.5}$ and PM_{10} were 91.4 (72.7–108.8), 5.0 (2.3–7.8), 0.24 (0.05–0.48), 1.43 (0.53–2.35), 0.23 (0.05–0.45), 0.09 (0.05–0.17), 0.03 (0.01–0.05), 0.04 (0.01–0.08), 0.27 (0.07–0.49), 0.51 (0.19–0.84), and 0.57 (0.15–1.05) Tg yr^{-1}, respectively.

5 Conclusion

In this study, we developed a high-spatiotemporal-resolution (daily data in a 1 km×1 km grid) inventory of emissions from biomass burning in China based on MODIS FRP data. The annual average emissions of were 91.4 (72.7–108.8), 5.0 (2.3–7.8), 0.24 (0.05–0.48), 0.23 (0.05–0.45), 0.04 (0.01–0.08), 0.27 (0.07–0.49) and 0.51 (0.19–0.84) Tg yr^{-1} for CO_2, CO, CH_4, NO_x, BC, OC, and $PM_{2.5}$, respectively. On a national scale, forest fires contribute the largest portion (45 %) of total CO_2 emissions from open fires. Agricultural fires and grassland fires ranked for the second and third places, accounting for 39 % and 15 %, respectively. Emissions in southwestern China and northeastern China are determined to be primary contributor, accounting for 52 % of the total emission. Spatially, forest and grassland fires were concentrated in the northeast and south regions. Cropland fires extensively occurred in the Northeast China Plain, the North China Plain, and the Middle–Lower Yangtze Plain, and shrubland fires happened in the south region such as Guangdong and Yunnan province. Temporally, total emissions were relatively high in 2003 and 2014, and the lowest emissions occurred in 2016. Most wild fires, including forest, grassland and shrubland, occurred during dry season (October to March of the following year), whereas agricultural fires were concentrated in the harvest season (June and October). Compared with estimations by other methods, our results are much higher than those obtained from the burned area method as the FRE method avoids uncertainties cause by inaccuracy of satellite-derived burned area and multiple other parameters. Our estimates were very close to those from GFED4s and GFASv1.0, as well as grassland and cropland fire emissions from FINNv1.5, indicating that our results were reasonable and can be used for further research. Furthermore, the temporal and spatial resolution of our inventory (daily, 1 km) are higher than that of GFED4s (monthly, 0.25 degrees) and GFASV1.0 (daily, 0.5 degrees). Uncertainties in our estimates may have been caused by many factors such as the characterization of the fire energy radiative diurnal cycle; thus, future studies should seek to improve the accuracy of the method.

Data availability. MODIS data can be freely accessed at https://search.earthdata.nasa.gov/search. GlobeLand30 data are downloaded from http://www.globallandcover.com/GLC30Download/index.aspx. GFASv1.0 data are available on http://apps.ecmwf.int/datasets/data/cams-gfas/. GFED4s data can be downloaded from https://daac.ornl.gov/VEGETATION/guides/fire_emissions_v4.html. FINNv1.5 data can be found at http://bai.acom.ucar.edu/Data/fire/.

Author contributions. This work was designed by YS and performed by LY, PD, MZ, ML, and TX. LY and YS led the writing of the papers and prepared the figures with contributions from all co-authors.

Competing interests. The authors declare that they have no conflict of interest.

Acknowledgements. The MODIS Thermal Anomalies/Fire products (MOD14/MYD14) and burned area product (MCD64A1) were provided by Land Process Distributed Active Archive Center (LPDAAC), USA. The GlobeLand30 land cover dataset was provided by the National Geomatics Center of China. This study was funded by National Key R&D Program of China (2016YFC0201505) and National Natural Science Foundation of China (NSFC) (91644212 and 41675142).

References

Andreae, M., Fishman, J., Garstang, M., Goldammer, J., Justice, C., Levine, J., Scholes, R., Stocks, B., Thompson, A., and Van Wilgen, B.: Biomass Burning in the Global Environment: First Results from the IGAC/BIBEX Field Campaign STARE/TRACE-A/SAFARI-92, in: Global atmospheric-biospheric chemistry, Springer, 83-101, 1994.

Andreae, M. O.: Biomass burning: its history, use, and distribution and its impact. Global Biomass Burning: Atmospheric, Climatic, and Biospheric Implications [JS Levine (Ed.)]. Cambridge, MA, MIT Press, 1991.

Bond, N. A., Cronin, M. F., Freeland, H., and Mantua, N.: Causes and impacts of the 2014 warm anomaly in the NE Pacific, Geophysical Research Letters, 42, 3414-3420, 2015.

Bond, T. C., Streets, D. G., Yarber, K. F., Nelson, S. M., Woo, J.-H., and Klimont, Z.: A technology-based global inventory of black and organic carbon emissions from combustion, Journal of Geophysical Research: Atmospheres, 109, 10.1029/2003JD003697, 2004.

Chen, J., Li, C., Ristovski, Z., Milic, A., Gu, Y., Islam, M. S., Wang, S., Hao, J., Zhang, H., He, C., Guo, H., Fu, H., Miljevic, B., Morawska, L., Thai, P., Lam, Y. F., Pereira, G., Ding, A., Huang, X., and Dumka, U. C.: A review of biomass burning: Emissions and impacts on air quality, health and climate in China, Science of The Total Environment, 579, 1000-1034, https://doi.org/10.1016/j.scitotenv.2016.11.025, 2017a.

Chen, J., Liao, A., Chen, J., Peng, S., Chen, l., and Zhang, h.: 30-Meter Global Land Cover Data Product- Globe Land30, Geomatics World, 24, 1-8, 2017b.

Crutzen, P. J., Heidt, L. E., Krasnec, J. P., Pollock, W. H., and Seiler, W.: Biomass burning as a source of atmospheric gases CO, H2, N2O, NO, CH3Cl and COS, Nature, 282, 253, 1979.

Freeborn, P. H., Wooster, M. J., Hao, W. M., Ryan, C. A., Nordgren, B. L., Baker, S. P., and Ichoku, C.: Relationships between energy release, fuel mass loss, and trace gas and aerosol emissions during laboratory biomass fires, Journal of Geophysical Research, 113, 10.1029/2007jd008679, 2008.

Gao, X., Ma, W., Ma, C., Zhang, F., and Wang, Y.: Analysis on the current status of utilization of crop straw in China (in Chinese), 242-247 pp., 2002.

Huang, X., Li, M., Friedli, H. R., Song, Y., Chang, D., and Zhu, L.: Mercury emissions from biomass burning in China, Environmental science & technology, 45, 9442-9448, 2011.

Huang, X., Li, M., Li, J., and Song, Y.: A high-resolution emission inventory of crop burning in fields in China based on MODIS Thermal Anomalies/Fire products, Atmospheric Environment, 50, 9-15, 2012.

Jian, W., Kong, S., Wu, F., Yi, C., Zheng, S., Qin, Y., Huang, Z., Yang, G., Zheng, M., and Liu, D.: Estimating the open biomass burning emissions in Central and Eastern China from 2003 to 2015 based on satellite observation, Atmospheric Chemistry & Physics, 1-49, 2018.

Jin, Q., Ma, X., Wang, G., Yang, X., and Guo, F.: Dynamics of major air pollutants from crop residue burning in mainland China, 2000–2014, Journal of Environmental Sciences, 70, 190-205, 2018.

Kaiser, J., Heil, A., Andreae, M., Benedetti, A., Chubarova, N., Jones, L., Morcrette, J., Razinger, M., Schultz, M., and Suttie, M.: Biomass burning emissions estimated with a global fire assimilation system based on observed fire radiative power, 2012.

Kaufman, Y. J., Remer, L., Ottmar, R., Ward, D., Li, R. R., Kleidman, R., Fraser, R. S., Flynn, L., McDougal, D., and Shelton, G.: Relationship between remotely sensed fire intensity and rate of emission of smoke: SCAR-C experiment, Global biomass burning, 685-696, 1996.

Li, J., Song, Y., Huang, X., and Li, M.: Comparison of forest burned areas in mainland China derived from MCD45A1 and data recorded in yearbooks from 2001 to 2011, International Journal of Wildland Fire, 24, 103-113, 2015.

Li, J., Bo, Y., and Xie, S.: Estimating emissions from crop residue open burning in China based on statistics and MODIS fire products, Journal of Environmental Sciences, 44, 158-170, https://doi.org/10.1016/j.jes.2015.08.024, 2016a.

Li, J., Li, Y., Bo, Y., and Xie, S.: High-resolution historical emission inventories of crop residue burning in fields in China for the period 1990–2013, Atmospheric Environment, 138, 152-161, 2016b.

Liu, M., Song, Y., Yao, H., Kang, Y., Li, M., Huang, X., and Hu, M.: Estimating emissions from agricultural fires in the North China Plain based on MODIS fire radiative power, Atmospheric Environment, 112, 326-334, 10.1016/j.atmosenv.2015.04.058, 2015.

Lu, A., Tian, H., Liu, M., Liu, J., and Melillo, J. M.: Spatial and temporal patterns of carbon emissions from forest fire in China from 1950 to 2000, Journal of Geophysical Research Atmospheres, 111, -, 2006.

McCarty, J. L., Ellicott, E. A., Romanenkov, V., Rukhovitch, D., and Koroleva, P.: Multi-year black carbon emissions from cropland burning in the Russian Federation, Atmospheric Environment, 63, 223-238, https://doi.org/10.1016/j.atmosenv.2012.08.053, 2012.

Mehmood, K., Chang, S., Yu, S., Wang, L., Li, P., Li, Z., Liu, W., Rosenfeld, D., and Seinfeld, J. H.: Spatial and temporal distributions of air pollutant emissions from open crop straw and biomass burnings in China from 2002 to 2016, Environmental Chemistry Letters, 16, 301-309, 2018.

Moreira de Araújo, F., Ferreira, L. G., and Arantes, A. E.: Distribution Patterns of Burned Areas in the Brazilian Biomes: An Analysis Based on Satellite Data for the 2002–2010 Period, Remote Sensing, 4, 1929-1946, 10.3390/rs4071929, 2012.

Ni, H., Han, Y., Cao, J., Chen, L. W. A., Tian, J., Wang, X., Chow, J. C., Watson, J. G., Wang, Q., Wang, P., Li, H., and Huang, R.-J.: Emission characteristics of carbonaceous particles and trace gases from open burning of crop residues in China, Atmospheric Environment, 123, 399-406, https://doi.org/10.1016/j.atmosenv.2015.05.007, 2015.

Qiu, X., Duan, L., Chai, F., Wang, S., Yu, Q., and Wang, S.: Deriving High-Resolution Emission Inventory of Open Biomass Burning in China based on Satellite Observations, Environ Sci Technol, 50, 11779-11786, 10.1021/acs.est.6b02705, 2016.

Reid, J., Koppmann, R., Eck, T., and Eleuterio, D.: A review of biomass burning emissions part II: intensive physical properties of biomass burning particles, Atmospheric Chemistry and Physics, 5, 799-825, 2005.

Roy, D. P., Boschetti, L., Justice, C. O., and Ju, J.: The collection 5 MODIS burned area product — Global evaluation by comparison with the MODIS active fire product, Remote Sensing of Environment, 112, 3690-3707, 10.1016/j.rse.2008.05.013, 2008.

Roy, D. P., and Boschetti, L.: Southern Africa Validation of the MODIS, L3JRC, and GlobCarbon Burned-Area Products, IEEE Transactions on Geoscience and Remote Sensing, 47, 1032-1044, 10.1109/tgrs.2008.2009000, 2009.

Seiler, W., and Crutzen, P. J.: Estimates of gross and net fluxes of carbon between the biosphere and the atmosphere from biomass burning, Climatic Change, 2, 207-247, 10.1007/bf00137988, 1980.

Song, Y., Liu, B., Miao, W., Chang, D., and Zhang, Y.: Spatiotemporal variation in nonagricultural open fire emissions in China from 2000 to 2007, Global biogeochemical cycles, 23, 2009.

Song, Y., Chang, D., Liu, B., Miao, W., Zhu, L., and Zhang, Y.: A new emission inventory for nonagricultural open fires in Asia from 2000 to 2009, Environmental Research Letters, 5, 014014, 10.1088/1748-9326/5/1/014014, 2010.

Streets, D., Yarber, K., Woo, J. H., and Carmichael, G.: Biomass burning in Asia: Annual and seasonal estimates and atmospheric emissions, Global Biogeochemical Cycles, 17, 2003.

Tao, S., Ru, M. Y., Du, W., Zhu, X., Zhong, Q. R., Li, B. G., Shen, G. F., Pan, X. L., Meng, W. J., Chen, Y. L., Shen, H. Z., Lin, N., Su, S., Zhuo, S. J., Huang, T. B., Xu, Y., Yun, X., Liu, J. F., Wang, X. L., Liu, W. X., Cheng, H. F., and Zhu, D. Q.: Quantifying the rural residential energy transition in China from 1992 to 2012 through a representative national survey, Nature Energy, 3, 567-573, 10.1038/s41560-018-0158-4, 2018.

Vadrevu, K. P., Ellicott, E., Badarinath, K. V. S., and Vermote, E.: MODIS derived fire characteristics and aerosol optical depth variations during the agricultural residue burning season, north India, Environmental Pollution, 159, 1560-1569, https://doi.org/10.1016/j.envpol.2011.03.001, 2011.

Van Der Werf, G. R., Randerson, J. T., Giglio, L., Van Leeuwen, T. T., Chen, Y., Rogers, B. M., Mu, M., Van Marle, M. J., Morton, D. C., and Collatz, G. J.: Global fire emissions estimates during 1997-2016, 2017.

Vermote, E., Ellicott, E., Dubovik, O., Lapyonok, T., Chin, M., Giglio, L., and Roberts, G. J.: An approach to estimate global biomass burning emissions of organic and black carbon from MODIS fire radiative power, Journal of Geophysical Research, 114, 10.1029/2008jd011188, 2009.

Wiedinmyer, C., Akagi, S., Yokelson, R. J., Emmons, L., Al-Saadi, J., Orlando, J., and Soja, A.: The Fire INventory from

NCAR (FINN): A high resolution global model to estimate the emissions from open burning, Geoscientific Model Development, 4, 625, 2011.

Wooster, M. J.: Small-scale experimental testing of fire radiative energy for quantifying mass combusted in natural vegetation fires, Geophysical Research Letters, 29, 23-21-23-24, 2002.

Wooster, M. J., Roberts, G., Perry, G. L. W., and Kaufman, Y. J.: Retrieval of biomass combustion rates and totals from fire radiative power observations: FRP derivation and calibration relationships between biomass consumption and fire radiative energy release, Journal of Geophysical Research, 110, 10.1029/2005jd006318, 2005.

Yan, X., Ohara, T., and Akimoto, H.: Bottom-up estimate of biomass burning in mainland China, Atmospheric Environment, 40, 5262-5273, 10.1016/j.atmosenv.2006.04.040, 2006.

Yang, S., He, H., Lu, S., Chen, D., and Zhu, J.: Quantification of crop residue burning in the field and its influence on ambient air quality in Suqian, China, Atmospheric Environment, 42, 1961-1969, https://doi.org/10.1016/j.atmosenv.2007.12.007, 2008.

Zhou, Y., Xing, X., Lang, J., Chen, D., Cheng, S., Lin, W., Xiao, W., and Liu, C.: A comprehensive biomass burning emission inventory with high spatial and temporal resolution in China, Atmospheric Chemistry and Physics, 17, 2839, 2017.

Table 1. Biomass burning emissions inventory (Tg) of China from 2003 to 2017.

Year	CO_2	CO	CH_4	NMHC	NO_x	NH_3	SO_2	BC	OC	$PM_{2.5}$	PM_{10}
2003	123.0	6.4	0.27	1.18	0.27	0.09	0.04	0.05	0.42	0.75	0.84
2004	113.0	6.0	0.27	1.44	0.27	0.10	0.04	0.05	0.36	0.66	0.74
2005	74.6	4.1	0.19	1.12	0.18	0.07	0.02	0.03	0.22	0.42	0.47
2006	91.6	4.9	0.22	1.22	0.22	0.08	0.03	0.04	0.29	0.53	0.59
2007	84.2	4.6	0.22	1.30	0.21	0.08	0.03	0.04	0.26	0.48	0.53
2008	97.6	5.2	0.23	1.22	0.23	0.08	0.03	0.04	0.32	0.59	0.64
2009	101.3	5.4	0.24	1.30	0.24	0.09	0.03	0.04	0.33	0.60	0.66
2010	87.4	4.7	0.22	1.24	0.21	0.08	0.03	0.04	0.27	0.50	0.55
2011	77.2	4.3	0.20	1.27	0.20	0.07	0.02	0.03	0.22	0.42	0.47
2012	81.1	4.6	0.23	1.57	0.22	0.08	0.02	0.04	0.21	0.41	0.47
2013	93.2	5.2	0.24	1.49	0.24	0.09	0.03	0.04	0.26	0.50	0.57
2014	117.3	6.6	0.33	2.16	0.31	0.12	0.03	0.05	0.31	0.61	0.69
2015	94.8	5.5	0.28	2.03	0.27	0.10	0.03	0.04	0.22	0.46	0.53
2016	59.8	3.4	0.17	1.20	0.17	0.06	0.02	0.03	0.14	0.30	0.34
2017	75.1	4.4	0.23	1.66	0.22	0.08	0.02	0.03	0.17	0.36	0.41
Average	91.4	5.0	0.24	1.43	0.23	0.09	0.03	0.04	0.27	0.51	0.57

Table 2. Average biomass burning emissions (Gg) in each province from 2003 to 2017.

region/province	CO_2	CO	CH_4	NMHC	NO_x	NH_3	SO_2	BC	OC	$PM_{2.5}$	PM_{10}
Northwest	2607.4	154.9	8.1	60.8	7.8	2.9	0.7	1.2	4.8	11.0	13.4
Xinjiang	1207.2	72.6	3.9	29.7	3.7	1.4	0.3	0.5	2.0	4.8	6.0
Gansu	359.0	21.1	1.1	8.0	1.1	0.4	0.1	0.2	0.7	1.6	1.9
Ningxia	211.7	13.0	0.7	5.6	0.7	0.3	0.1	0.1	0.3	0.8	1.0
Qinghai	131.4	7.5	0.4	2.5	0.4	0.1	0.0	0.1	0.2	0.5	0.7
Shaanxi	698.0	40.8	2.1	15.0	2.0	0.8	0.2	0.3	1.5	3.3	3.8
Northeast	23524.0	1323.4	64.8	416.9	63.6	22.8	6.9	10.2	56.9	114.6	136.0
Inner Mongolia	5769.3	307.0	14.1	70.5	14.5	4.6	1.8	2.3	15.0	28.5	35.3
Heilongjiang	13812.4	775.1	37.7	241.7	36.8	13.4	4.1	6.1	34.9	69.5	81.1
Jilin	2394.4	148.4	8.1	67.0	7.6	3.0	0.6	1.1	3.9	9.8	11.6
Liaoning	1548.0	92.9	4.9	37.8	4.6	1.8	0.4	0.7	3.0	6.9	8.1
North	8336.8	516.3	28.2	232.4	26.2	10.5	2.2	4.0	14.8	35.8	41.2
Beijing	146.2	8.8	0.5	3.7	0.4	0.2	0.0	0.1	0.3	0.7	0.8
Shanxi	1153.7	66.6	3.4	23.5	3.3	1.2	0.3	0.5	2.5	5.4	6.4
Hebei	1592.5	97.3	5.2	42.0	4.9	1.9	0.4	0.8	2.9	6.9	8.0
Shandong	2258.5	143.6	8.0	69.5	7.4	3.0	0.6	1.1	3.5	9.2	10.5
Tianjin	205.2	13.2	0.7	6.6	0.7	0.3	0.1	0.1	0.3	0.8	0.9
Henan	2980.8	186.9	10.3	87.1	9.5	3.9	0.8	1.5	5.2	12.8	14.5
Central	15299.8	844.0	39.7	243.6	37.9	14.6	4.7	7.0	47.1	88.4	96.7
Hubei	1832.6	102.9	5.0	32.4	4.7	1.8	0.6	0.9	5.3	10.3	11.3
Anhui	4227.0	262.6	14.3	119.5	13.2	5.4	1.1	2.1	7.9	18.8	21.1
Hunan	5240.9	271.7	11.6	52.5	11.4	4.2	1.7	2.3	19.0	33.4	36.3
Jiangxi	3999.2	206.8	8.8	39.3	8.6	3.2	1.3	1.8	14.8	25.9	28.0
Southwest	25603.5	1326.1	56.6	249.8	55.8	20.1	8.4	11.1	92.0	160.4	175.1
Xizang	1993.7	100.2	4.1	14.3	4.1	1.4	0.7	0.9	7.7	13.1	14.3
Sichuan	2531.7	134.9	6.1	30.1	6.1	2.0	0.8	1.0	7.6	13.4	15.5

Table 2. Continued.

region/province	CO_2	CO	CH_4	NMHC	NO_x	NH_3	SO_2	BC	OC	$PM_{2.5}$	PM_{10}
Chongqing	261.0	15.8	0.8	6.7	0.8	0.3	0.1	0.1	0.5	1.2	1.4
Yunnan	10335.9	538.8	23.2	106.5	22.9	8.2	3.4	4.5	36.5	63.8	69.7
Guizhou	2460.2	126.1	5.4	21.8	5.5	1.8	0.8	1.0	8.2	14.5	16.6
Guangxi	8021.1	410.1	17.0	70.5	16.5	6.2	2.7	3.6	31.6	54.4	57.6
Southeast	16046.3	868.4	39.7	224.7	38.3	14.5	5.1	7.2	51.9	95.1	103.9
Jiangsu	2587.7	166.3	9.4	82.8	8.6	3.6	0.7	1.3	3.8	10.3	11.8
Shanghai	112.5	7.2	0.4	3.6	0.4	0.2	0.0	0.1	0.2	0.4	0.5
Zhejiang	1515.8	86.1	4.2	28.4	4.0	1.6	0.5	0.7	4.2	8.3	9.1
Fujian	3428.0	176.0	7.4	31.4	7.2	2.7	1.1	1.5	13.0	22.6	24.3
Guangdong	7659.7	392.9	16.5	68.5	16.3	5.9	2.5	3.3	28.2	48.9	53.3
Macao	0.5	0.0	0.0	0.0	0.0	0.0	0.0	0.0	0.0	0.0	0.0
Hong Kong	24.7	1.2	0.0	0.1	0.0	0.0	0.0	0.0	0.1	0.2	0.2
Hainan	515.6	27.1	1.2	5.8	1.1	0.4	0.2	0.2	1.9	3.4	3.6
Taiwan	201.7	11.5	0.6	3.9	0.6	0.2	0.1	0.1	0.5	1.0	1.1

Table 3. Comparison of annual mean CO_2 emissions (Tg) from biomass burning calculated in our study with estimates made by other methods.

Year	This study	MCD64A1[a]	GFED4s[b]	GFASv1[c]	FINNv1.5[d]
2003	123.0	21.4	112.9	138.6	161.2
2004	113.0	10.7	104.5	90.3	176.4
2005	74.6	9.5	71.9	67.0	157.1
2006	91.6	11.2	91.5	76.1	185.5
2007	84.2	11.4	90.0	78.3	196.2
2008	97.6	25.1	122.4	96.3	217.1
2009	101.3	15.1	100.3	77.8	256.3
2010	87.4	12.3	80.8	76.1	213.4
2011	77.2	9.4	94.8	63.3	188.0
2012	81.1	10.9	77.5	74.0	223.3
2013	93.2	9.6	74.9	61.5	221.9
2014	117.3	20.8	114.3		157.4
2015	94.8	14.8	105.5		122.2
2016	59.8	7.4	79.3		175.7
2017	75.1	16.3			
Average	91.4	13.5	95.5	81.7	189.4

[a] Estimations based on MODIS burned area product (MCD64A1).

[b] GEFD4s estimated emissions based on burned area boosted by small fires burned area (Van Der Werf et al., 2017).

[c] GFASv1 calculated emissions with a global fire assimilation system based on FRP (Kaiser et al., 2012).

[d] FINNv1.5 was established by using fire count method (Wiedinmyer et al., 2011).

Table 4. Comparison of annual average CO_2 emissions (Tg) from each fire type calculated in our study with estimates made by other methods.

	Forest	Grassland	Shrubland	Cropland
This study	40.8	14.1	1.2	35.3
Huang et al. (2012)[a]				68.0
Yan et al. (2006)[a]	3.4	0.3		185.0
MCD64A1[b]	6.0	4.4	0.8	2.5
GFED4s[b]	36.2	19.7		38.2
FINNv1.5[b]	105.4	14.5	31.4	38.1

[a] Emissions estimated by using statistical data.

[b] Refer to Table 3.

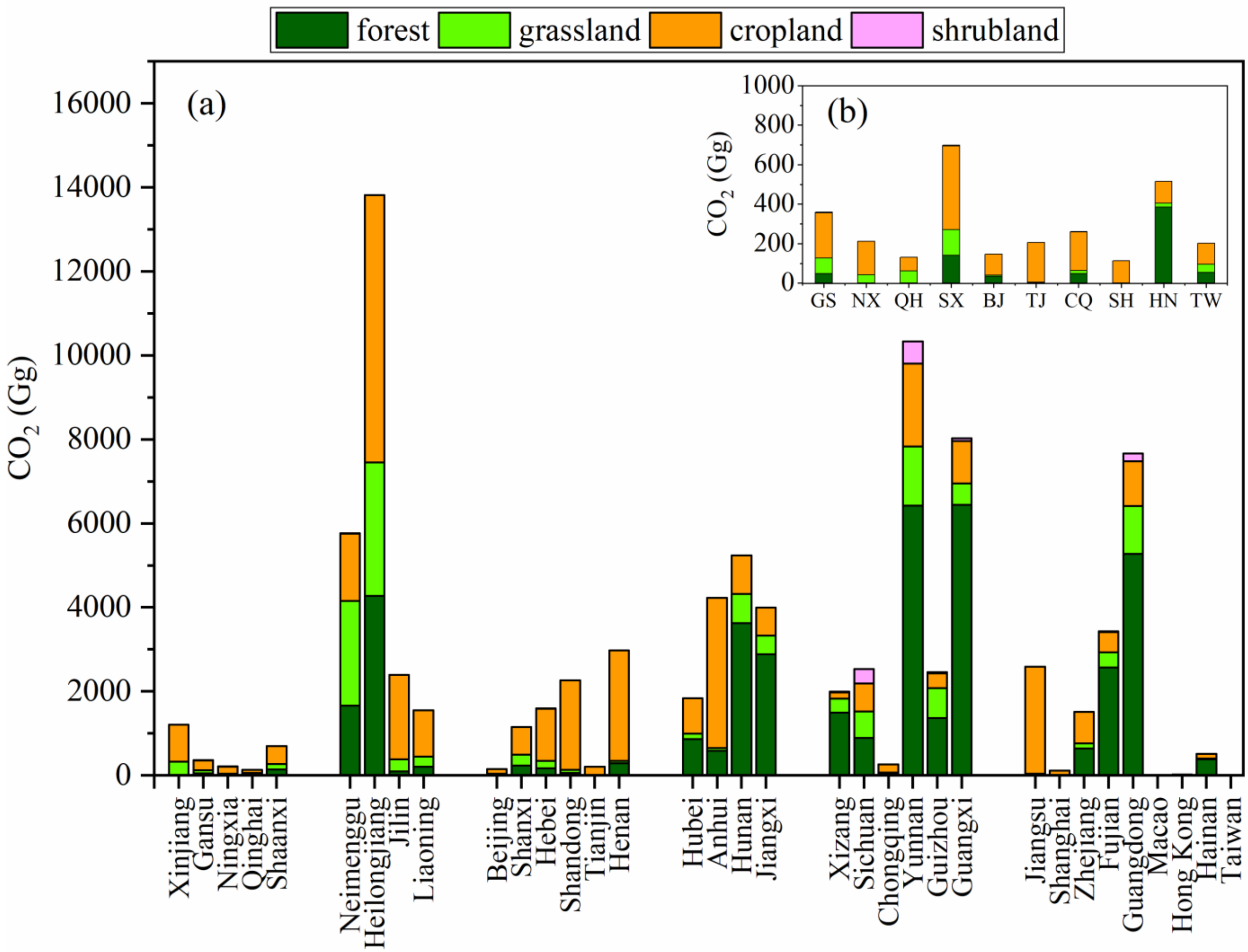

Figure 1. (a) Source-specific CO_2 emission in each province. Each group of bars represent a region (from left to right): Northwest (Xinjiang–Shaanxi), Northeast (Neimenggu–Liaoning), North (Beijing–Henan), Central (Hubei–Jiangxi), Southwest (Xizang–Guangxi), Southeast (Jiangsu–Taiwan). **Ten provinces and municipalities with emissions lower than 1000 Gg yr^{-1} were shown in detail in (b)**: Gansu (GS), Ningxia (NX), Qinghai (QH), Shaanxi (SX), Beijing (BJ), Tianjin (TJ), Chongqing (CQ), Shanghai (SH), Hainan (HN) and Taiwan (TW). Macao and Hong Kong have minimal emissions, that is 0.5 Gg in Macao, consisting of 0.4 Gg from forest fires and 0.1 Gg from grassland fires; and 24.7 Gg in Hong Kong, consisting of 20.6 Gg (83 %) from forest fires, 2.7 Gg (11 %) from grassland fires, 0.7 Gg from shrubland and 0.7 Gg from cropland fires.

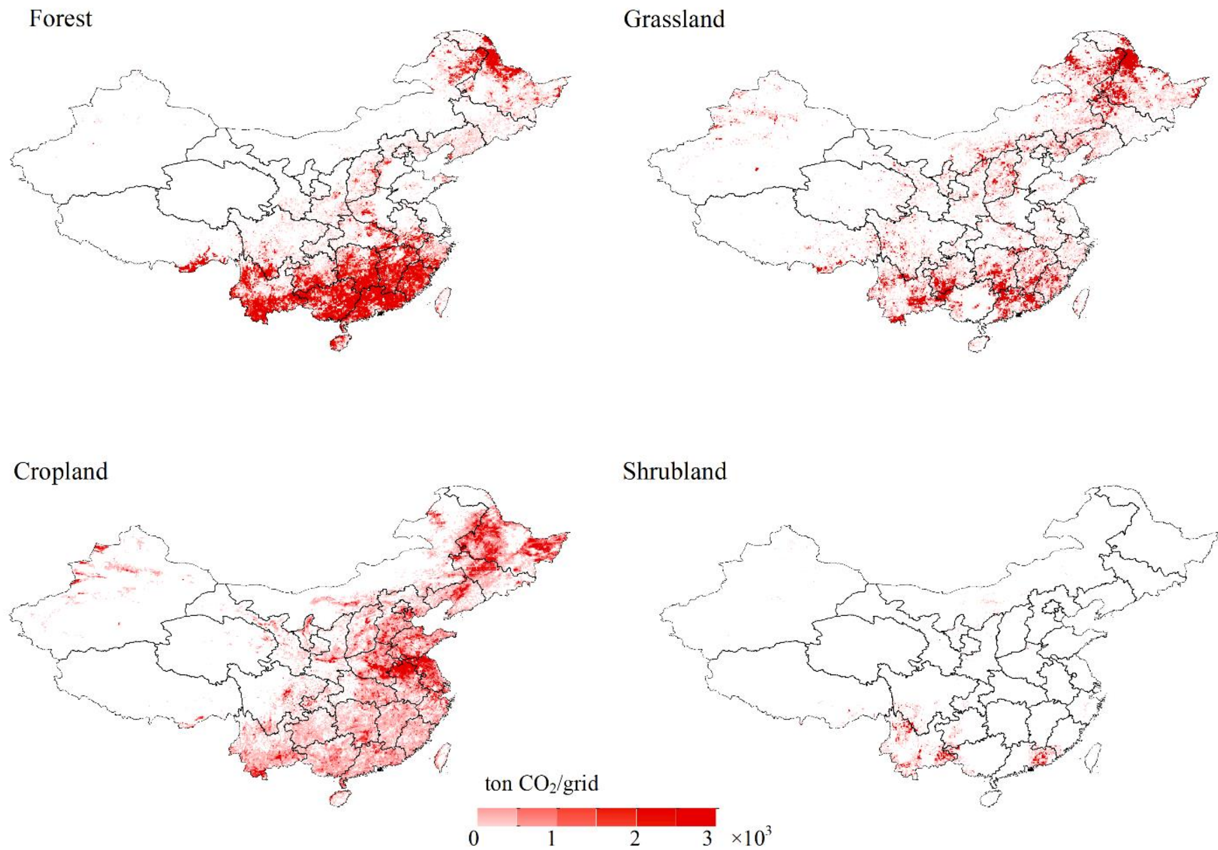

Figure 2. Spatial distribution of CO_2 emissions (ton) from each land cover type (excluding small islands in the South China Sea).

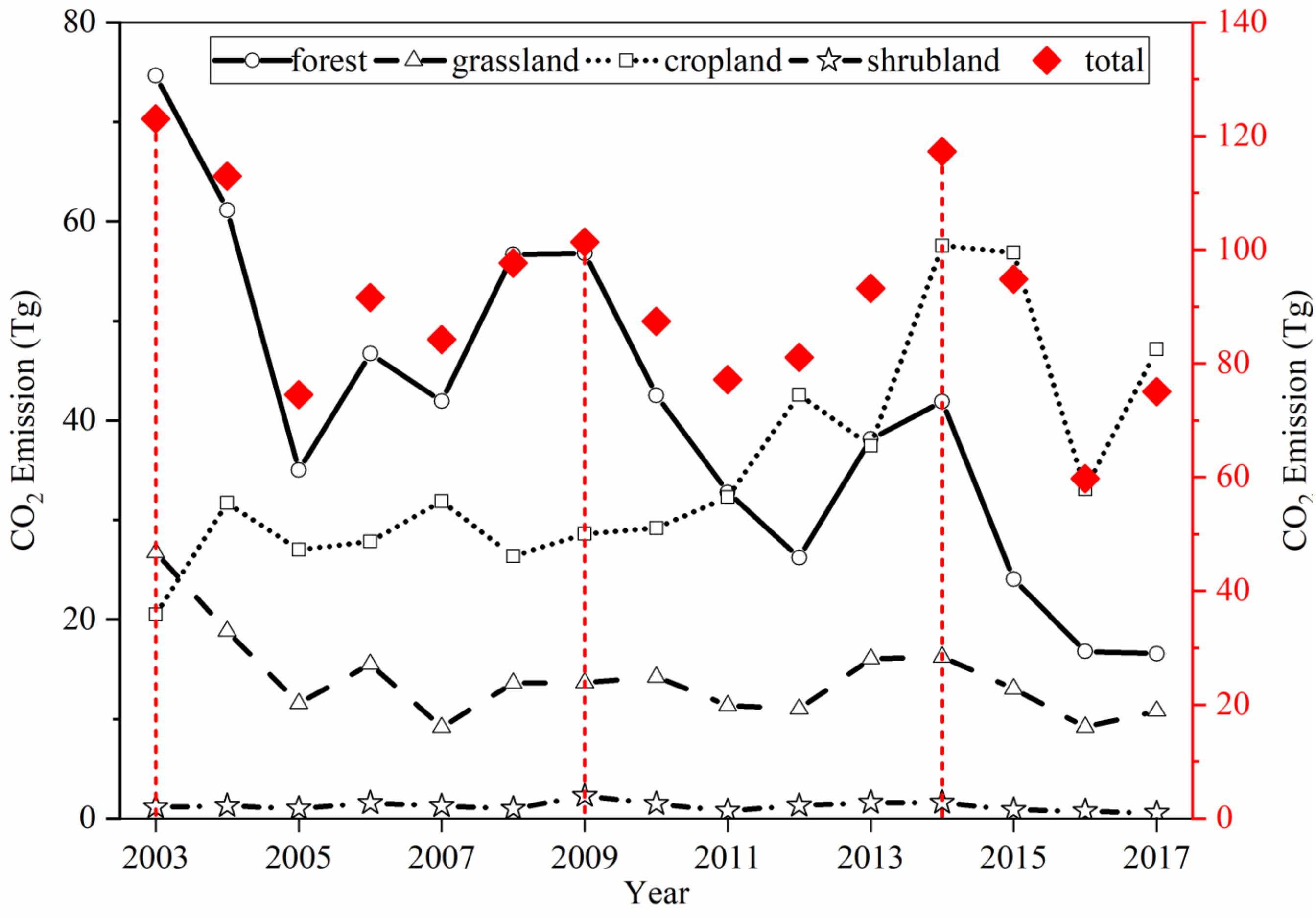

Figure 3. Annual variation in total and source-specific CO_2 emissions (Tg), 2003–2017

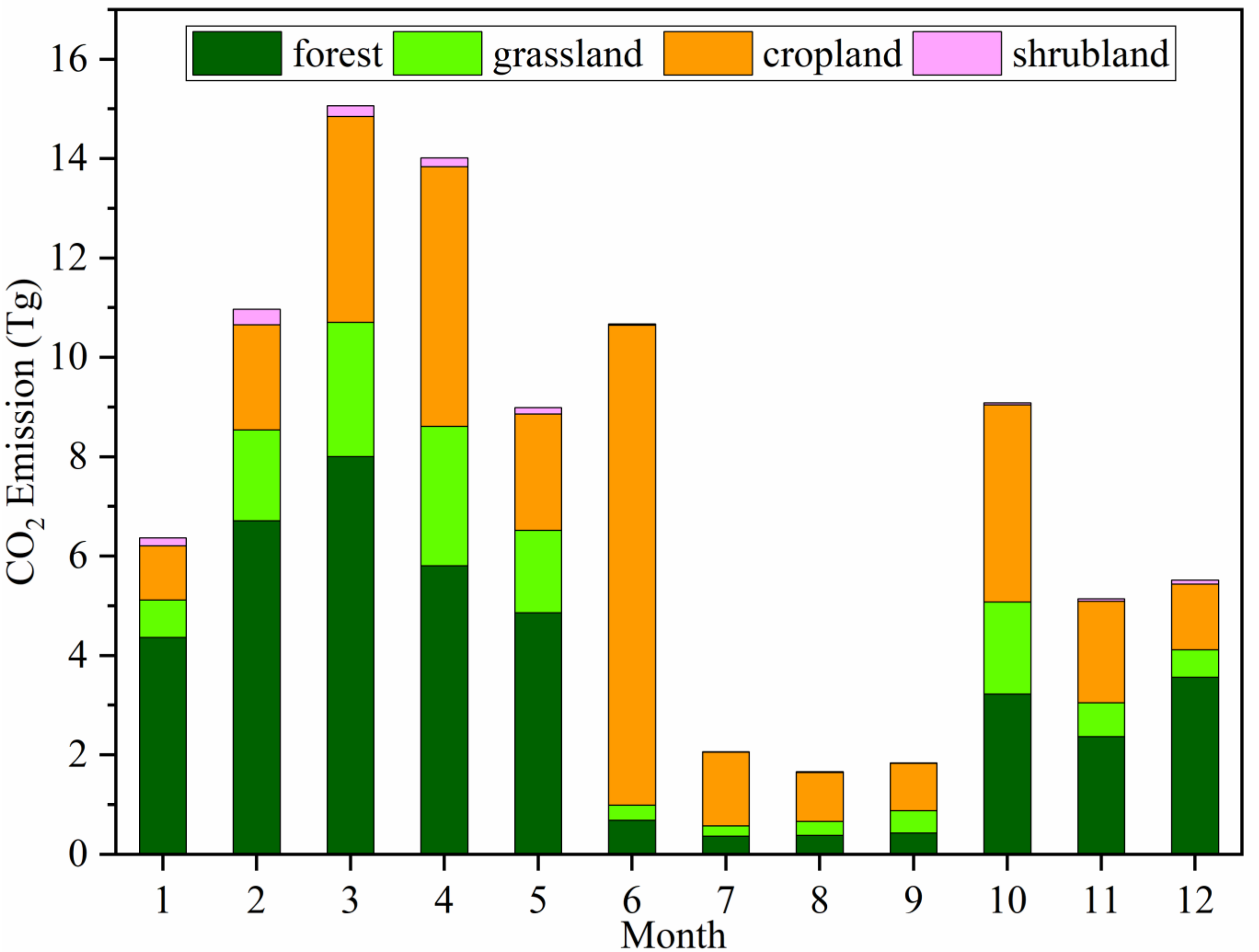

Figure 4. Monthly distributions of source-specific CO_2 emissions (Tg) in China.